Influence of thermal stress on temperature sensitivity of FBG-GFRP bars*

SUN Li(孙丽)[1,2]**, ZHAO Jian**(赵健)[1], **and LIANG De-zhi**(梁德志)[1]

1. School of Civil Engineering, Shenyang Jianzhu University, Shenyang 110168, China

2. School of Civil and Hydraulic Engineering, Dalian University of Technology, Dalian 116023, China

(Received 1 April 2011)

The influence of thermal stress on the temperature sensitivity of fiber Bragg grating-glass fiber reinforce polymer (FBG-GFRP) bars is studied by three methods, namely, direct experimental calibration method, stress analysis (finite element analysis) method and the method of apparent temperature sensitivity coefficient. In comparison with the other two methods, fewer parameters are required and the calculation is simple in the method of apparent temperature sensitivity coefficient, while the analytical error is limited within 2%. It is concluded that the results of the method of apparent temperature sensitivity coefficient could be good reference for engineering applications.

Document code: A **Article ID:** 1673-1905(2011)04-0269-4

DOI 10.1007/s11801-011-9226-8

At present, fiber Bragg grating (FBG) sensor is the first choice for structural health monitoring due to its advantages, such as anti-electromagnetic interference, small size, quasi-distributed sensing, corrosion-proof and absolute measurement, etc[1-3]. Smart glass fiber reinforce polymer (GFRP) bar was developed by Kalamkarov et al[4] through embedding FBG sensors in a GFRP bar to combine the reinforcement function and the sensing function together in concrete structures. When the temperature fluctuation occurs, the thermal stress is induced by thermal mismatch due to the difference of the thermal expansion coefficients between the optical fiber and the matrix material. Therefore, FBG is highly sensitive not only to strain (as designed), but also to temperature fluctuation. Numerous studies have been carried out to separate these two effects and/or to find a way for temperature compensation[5-8], but the influence of thermal stress on temperature sensitivity of FBG is rarely studied.

In this paper, stresses on all directions in FBG embedded in the matrix material are analyzed. With the finite element software we can calculate stresses in FBG, and emulation data is obtained to quest the temperature sensitivity coefficient of smart GFRP bar. Moreover, the approximate formula is derived for the simplification of calculation and the convenience of application.

In working environment, due to the mismatch of the thermal expansion coefficient, FBG is under stresses from the matrix material in both axial and radial directions, resulting in additional drift from the central wavelength of FBG. Generally, the influence of temperature on the central wavelength of FBG could be divided into three cases: wavelength drift caused by thermo-optic effect and thermal expansion $\Delta\lambda_{B1}$, wavelength drift caused by axial stress $\Delta\lambda_{B2}$, and wavelength drift caused by radial stress $\Delta\lambda_{B3}$. According to Ref.[9], the total wavelength drift can be regarded as the superposition of these three cases, that is: $\Delta\lambda_B = \Delta\lambda_{B1} + \Delta\lambda_{B2} + \Delta\lambda_{B3}$.

When temperature varies, the wavelength drift formula without considering the waveguide effect[9] is given by

$$\Delta\lambda_{B1} = \alpha_n \lambda_B \Delta T + \left\{ \varepsilon_{zz} - \frac{n_{eff}^2}{2}\left[(p_{11} + p_{12})\varepsilon_{rr} + p_{12}\varepsilon_{zz} \right] \right\} \lambda_B, \quad (1)$$

where α_n is the thermo-optic coefficient of FBG, λ_B is the central wavelength of FBG, p_{ij} is the elastic-optic coefficient of FBG, n_{eff} is the effective refractive index of FBG, and ε_{rr} and ε_{zz} are the radial and axial strains of FBG, respectively.

Under the state of free expansion, we have $\varepsilon_{rr}=\varepsilon_{\theta\theta}=\varepsilon_{zz}=\alpha_1\Delta T$, where α_1 is the linear expansion coefficient of FBG. Substituting $\varepsilon_{rr}=\varepsilon_{\theta\theta}=\varepsilon_{zz}=\alpha_1\Delta T$ into Eq.(1), the FBG wavelength drift formula under free expansion state is given as follows

* This work has been supported by the National Natural Science Foundation of China (No.10902073), the Science Foundation of Construction Ministry (No.2010-K2-21) and the Shenyang City Science Foundation of China (No.1081271-9-00).

** E-mail: sunli2001@hotmail.com

$$\Delta\lambda_{B1}=\alpha_n\lambda_B\Delta T+\left\{\alpha_1-\frac{n_{eff}^2}{2}[(p_{11}+2p_{12})\alpha_1]\right\}\lambda_B\Delta T. \quad (2)$$

The longitudinal strain sensitivity of the wavelength drift caused by homogeneous axial strain is given by[9]

$$\frac{\Delta\lambda_B}{\lambda_B}=\varepsilon_{zz}\left\{1-\frac{n_{eff}^2}{2}[p_{12}-(p_{11}+p_{12})\nu]\right\}, \quad (3)$$

where $\nu=\frac{\varepsilon_{rr}}{\varepsilon_{zz}}$ is the ratio of radial strain to axial strain.

Under the action of axial force P, the radial stress in the FBG is $\sigma_{rr}=\sigma_{\theta\theta}=0$, and the axial stress is $\sigma_{zz}=-P$. Thus, the stress components are given by $\varepsilon_{rr}=\varepsilon_{\theta\theta}=-\nu\varepsilon_{zz}$, $\varepsilon_{zz}=\sigma_{zz}/E_1$. Substituting the stress components into Eq.(3) yields

$$\Delta\lambda_{B2}=\frac{\sigma_{zz}\lambda_B}{E_1}\left\{1-\frac{n_{eff}^2}{2}[p_{12}-(p_{11}+p_{12})\nu_1]\right\}, \quad (4)$$

where E_1 and ν_1 are the modulus and the Poisson's ratio of FBG, respectively.

The internal stress state of FBG corresponding to the radial stress is $\sigma_{rr}=\sigma_{\theta\theta}\neq 0$, $\sigma_{zz}=0$. The corresponding strain state is given by $\varepsilon_{rr}=\varepsilon_{\theta\theta}=(1-\nu_1)\sigma_{rr}/E_1$, $\varepsilon_{zz}=-2\sigma_{rr}\nu_1/E_1$ and $\nu=\frac{\varepsilon_{rr}}{\varepsilon_{zz}}=\frac{-(1-\nu_1)}{\nu_1}$. Similarly, substituting the above equations into Eq.(3) yields

$$\Delta\lambda_{B3}=\frac{-\sigma_{rr}\lambda_B}{E_1}\left\{2\nu_1-\frac{n_{eff}^2}{2}[2\nu_1 p_{12}-(p_{11}+p_{12})(1-\nu_1)]\right\}. \quad (5)$$

In order to study the temperature sensitivity of FBG embedded in smart GFRP bar, we embed three FBGs whose central wavelength is 1573 nm in GFRP bars as shown in Fig.1. Temperature calibration is carried out to test the accuracy of the present method. The temperature response curve of FBG is shown in Fig.2.

Fig.1 Smart GFRP bars

In Fig.2 λ is the wavelength, T is the temperature and R is the correlation coefficient between the fitting curve and the raw data. Fig.2 presents excellent linear relationship between wavelength drift and temperature variation. The correlation coefficient R is above 99.99%. The calibrated temperature sensitivity coefficient is 17.6 pm/°C, which is about 1.67 times of that of bare fiber, namely, 10.53 pm/°C.

Based on the analysis above, the FBG central wavelength drift and the temperature sensitivity coefficient can be obtained by calculation. The finite element analysis is carried out to obtain the horizontal and axial stresses in the embedded FBG as temperature varies. 10 mm of the smart FBG-GFRP bar is selected to establish the finite element model, and material properties of the smart FBG-GFRP bar are as follows[10-13].

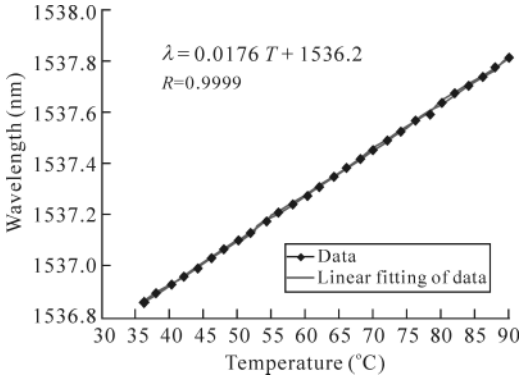

Fig.2 Temperature response curve of FBG embedded in smart GFRP bar

The parameters of GFRP bar are: radial temperature expansion coefficient $\alpha_{31}=33.7\times10^{-6}/°C$, axial temperature expansion coefficient $\alpha_{32}=6.58\times10^{-6}/°C$, Poisson's ratio $\nu_3=0.25$, Young's modulus $E_3=4\times10^{10}$ Pa, and radius $r_3=6$ mm. The parameters of the FBG cladding (polyimide) are: temperature expansion coefficient $\alpha_2=45\times10^{-6}/°C$, Poisson's ratio $\nu_2=0.335$, Young's modulus $E_2=3.5\times10^9$ Pa, and radius $r_2=125$ μm. The parameters of the core of FBG are: temperature expansion coefficient $\alpha_1=0.55\times10^{-6}/°C$, Poisson's ratio $\nu_1=0.17$, Young's modulus $E_1=7.2\times10^{10}$ Pa, radius $r_1=62.5$ μm, thermo-optic coefficient of FBG $\alpha_n=6.3\times10^{-6}/°C$, elastic-optic coefficient of FBG $p_{11}=0.121$, $p_{12}=0.27$, effective refractive index of FBG $n_{eff}=1.468$, and the central wavelength of FBG λ_B is 1537 nm. 20 °C as the initial temperature of all nodes is applied, while all the nodes are loaded by 30 °C to simulate the environment temperature, and finally we get the analysis results of radial and axial stresses on FBG embedded in GFRP bars. The radial stress is $\sigma_{rr}\approx\sigma_{\theta\theta}\approx4.1\times10^5\Delta T$ Pa, and the axial stress is $\sigma_{zz}\approx4.8\times10^6\Delta T$ Pa.

Substituting the FEM results into temperature sensitivity

calculation formula, the wavelength drift under the temperature load could be obtained as follows: ΔT = 10 °C, $\Delta\lambda_{B1}$ = 99.327 pm, $\Delta\lambda_{B2}$ = 80.041 pm and $\Delta\lambda_{B3}$ = -5.175 pm. Thus the total wavelength drift is $\Delta\lambda_B = \Delta\lambda_{B1} + \Delta\lambda_{B2} + \Delta\lambda_{B3}$ = 174.19 pm. Then the temperature sensitivity coefficient of smart GFRP bar is obtained as follows: $\Delta\lambda_B/\Delta T$ = 17.42 pm/°C, which is about 1.65 times of that of bare fiber, namely,10.53 pm/°C. The theoretical value is in good agreement with the calibrated value 17.6 pm/°C obtained by stress analysis above.

The theoretical analysis shows that temperature wavelength drift is mainly caused by the thermo-optic effect and thermal expansion, the axial stress and the radial stress. But the results reveal that the wavelength drift caused by the radial stress is only about 2.9% of the total. In engineering application, it is approximately believed that the wavelength drift is only caused by the thermo-optic effect and thermal expansion, as well as the axial stress. Therefore, the influence of temperature variation on the temperature sensitivity can be evaluated as follows.

As can be seen from Ref.[14], in temperature compensation, the reference temperature of FBG embedded in GFRP bar can be set as T_0 at first, and the GFRP bar is not loaded by any mechanical force. But when temperature varies, additional stress resulting from the thermal expansion mismatch between fiber and GFRP bar appears. The thermally induced axial stress can be expressed as

$$\Delta\sigma = E_F(\alpha_H - \alpha_\Lambda)\Delta T \ , \tag{6}$$

where E_F is Young's modulus of the fiber, α_H is thermal expansion coefficient of matrix material, and α_Λ is temperature expansion coefficient of the fiber.

On the substitution of Eq.(6), $\Delta\lambda_B$ is obtained as follows

$$\Delta\lambda_B = \lambda_B\left[\left(\left[\frac{\partial\varepsilon}{\partial\sigma}\right]_T + \frac{1}{n_{eff}}\left[\frac{\partial n_{eff}}{\partial\varepsilon}\right]_T\left[\frac{\partial\varepsilon}{\partial\sigma}\right]_T\right)\Delta\sigma + \left(\left[\frac{\partial\varepsilon}{\partial T}\right]_\sigma + \frac{1}{n_{eff}}\left[\frac{\partial n_{eff}}{\partial T}\right]_\sigma\right)\Delta T\right] \ . \tag{7}$$

Denote the sensitivity coefficient of stress as $S_\varepsilon \equiv \{1-p_e\} = \left\{1+\frac{1}{n_{eff}}\left[\frac{\partial n_{eff}}{\partial\varepsilon}\right]_T\right\}$, and the sensitivity coefficient of temperature as $S_T \equiv \{\alpha_\Lambda + \alpha_n\} = \left\{\frac{1}{\Lambda}\left[\frac{\partial\Lambda}{\partial T}\right]_\sigma + \frac{1}{n_{eff}}\left[\frac{\partial n_{eff}}{\partial T}\right]_\sigma\right\}$. Then

$$\frac{\Delta\lambda_B}{\lambda_B} = S_\varepsilon\left[\Delta\varepsilon + (\alpha_H - \alpha_\Lambda)\Delta T\right] + S_T\Delta T \ , \tag{8}$$

$$\frac{\Delta\lambda_B}{\lambda_B} = S_\varepsilon\Delta\varepsilon + \left[S_\varepsilon(\alpha_H - \alpha_\Lambda) + S_T\right]\Delta T \ . \tag{9}$$

The apparent temperature sensitivity coefficient S_a is introduced to calculate all the temperature factors causing the wavelength drift, namely, the thermo-optic effect and thermal expansion effect, and the axial stress as follows

$$S_a = S_T + S_\varepsilon(\alpha_H - \alpha_\Lambda) \ . \tag{10}$$

The thermally induced axial strain can be expressed as:

$$\Delta\varepsilon = \Delta\varepsilon_{12} + \Delta\varepsilon_{23} = (\alpha_3 - \alpha_2)\Delta T + (\alpha_2 - \alpha_1)\Delta T = (\alpha_3 - \alpha_1)\Delta T. \tag{11}$$

Therefore, the apparent temperature sensitivity coefficient of smart GFRP bar is

$$\Delta\lambda / \Delta T = S_a \times \lambda = \left[S_T + S_\varepsilon(\alpha_3 - \alpha_1)\right]\lambda. \tag{12}$$

The apparent temperature sensitivity obtained by the formula above is $\Delta\lambda/\Delta T = 10.53 + 1.2\times10^6 \times (6.58\times10^{-6} - 0.55\times10^{-6}) = 17.77$ pm/°C. Compared with the calculated value 17.412 pm /°C and the experimentally calibrated value 17.6 pm /°C, the error is less than 2%, which mainly results from the approximate treatment on the mechanical model. Therefore, Eq.(12) can be applied directly in engineering application to calculate the temperature sensitivity coefficient of smart GFRP bar.

In this paper, the additional stress in the FBG embedded in the GFRP bar is analyzed when the temperature varies, and the impact of additional stress on temperature sensitivity coefficient is obtained by further calculation. The temperature sensitivity coefficient 17.42 pm/°C is very close to the calibrated one, which validates the theoretical method. The apparent temperature sensitivity coefficient method is simple. The error, compared with the calculated value and the experimentally calibrated value, is less than 2%. Therefore, the presented method can provide reference for practical engineering applications.

References

[1] WU Yonghong, SHAO Changjiang, QU wenjun, ZHOU Wei and CAI Haiwen, Journal of Optoelectronics • Laser **21**, 481 (2010). (in Chinese)

[2] XIE Jianfeng, ZHANG Hua and SONG Lufa, Piezoelectrics and Acoustooptics **29**, 261 (2007). (in Chinese)

[3] WANG Yanlei, ZHOU Zhi, HAO Qingduo and OU Jinping, Journal of Optoelectronics • Laser **18**, 900 (2007). (in Chinese)

[4] Kalamkarov AL, Liu HQ and MacDonald DO, Comp. Part B **29B**, 21 (1998).

[5] JIA Zhen-an, QIAO Xue-guang and FU Hai-wei, Journal of Optoelectronics • Laser **14**, 453 (2003). (in Chinese)

[6] ZHANG Xiaojing, WU Zhanjun and ZHANG Boming, Journal of Optoelectronics • Laser **16**, 566 (2005). (in Chinese)

[7] LI Zhizhong, WANG Xin and YANG Huayong, Journal of Optoelectronics • Laser **17**, 1191 (2006). (in Chinese)

[8] XIE Jianfeng, ZHANG Hua, ZHANG Guoping, HU Ronghua and XU Jianning, Journal of Optoelectronics • Laser **19**, 1158 (2008). (in Chinese)

[9] XIE Jianfeng, ZHANG Hua and SONG Lufa, Microcomputer Information **23**, 150 (2007). (in Chinese)

[10] Fabiano Colpo, Laurent Humbert and John Botsis, Composites Science and Technology **67**, 1830 (2007).

[11] Kin-tak Lau, Zhou Limin and Tao Xiaoming, Composite Structures **58**, 39 (2002).

[12] Kin-tak Lau, Yuan Libo and Zhou Limin, Smart Materials and Structions **10**, 705 (2001).

[13] Giles C R, Journal of Lightwave Technology **15**, 1391 (1997).

[14] LI Chuan, ZHANG Yimo and ZHAO Yonggui, Fiber Grating: Principles, Techniques and Sensing Applications, Beijing: Sciencep, 163 (2005). (in Chinese)